PHYSICAL REVIEW B VOLUME 21, NUMBER 12 15 JUNE 1980

A computer model for amorphous FeF_3

M. E. Lines
Bell Laboratories, Murray Hill, New Jersey 07974
(Received 17 December 1979)

A computer model has been constructed for amorphous FeF_3 using a method involving the sequential addition of hard spheres of two different radii. A recognition of the effects of Coulomb forces is included by separating the ions of like charge as far as possible within the basic building scheme. A cluster sample of 858 ions has been produced and used to compute iron-iron, iron-fluorine, and fluorine-fluorine pair correlation functions, ion density, packing fractions, and such details of local configurational structure as the distribution of Fe–F–Fe bond angles θ. The electric field gradient distribution at the iron sites has been computed using a point-charge model and used to interpret the measured Mössbauer quadrupole spectra. Comparisons are made with the earlier model presented for amorphous yttrium iron garnet (YIG) and reveal subtle differences in the iron coordination between the two. It is suggested that whereas the dominant exchange energy in amorphous YIG comes via essentially contact Fe–anion–Fe nearest-neighbor bonds, well over half the magnetic energy in amorphous FeF_3 may come from "noncontact" bonds.

I. INTRODUCTION

The recent synthesis of a few magnetic noncrystalline insulators has added a new dimension to the study of amorphous magnetism. Earlier noncrystalline magnets had been metallic alloys with long-range exchange interactions and usually a broad distribution of magnetic moments. The noncrystalline insulators, such as FeF_2,[1] YIG,[2] and FeF_3,[3,4] are synthesized without the addition of extraneous glass-forming constituents and fall into an intermediate class of amorphous materials (loosely termed "ionic glasses") between metallic glasses, for which structural coordination numbers are largest, and covalent glasses (e.g., silicate glasses) for which the coordination numbers are smallest. In addition to representing a new class of amorphous materials, they hold particular interest since their magnetic properties are presumably dominated by interactions between near-neighbor magnetic cations and therefore directly reflect in some way local structure such as bond distances and angles. It therefore opens up the possibility of using magnetic experiments as probes of local coordination in the amorphous state.

The first requisite in such a project is a basic model which, it is hoped, can lead to some understanding of the grosser aspects of experimental observations and which can later be honed as the number of examples studied is increased. A first step in this direction was recently set out[5] for the case of amorphous yttrium iron garnet $Y_3Fe_5O_{12}$, commonly referred to as YIG. In Ref. 5 a computer model was constructed using a modification of the method pioneered by Bennett[6] based on the sequential addition of hard spheres. The modification allows for the presence of spheres of different radii corresponding to the different ion species present, and most importantly recognizes the presence of local Coulomb forces which are assumed to keep neighboring ions of like charge as far apart as the basic building algorithm will allow. Any tendencies toward directional (covalent) bonding are neglected.

In the present paper we use this technique to build a computer model for amorphous FeF_3. Cations can be separated by a distance $d = 2.7$ Å compared with $d = 2.4$ Å in YIG, and the model suggests a slight increase in density in passing to the amorphous phase in FeF_3 compared with a decrease in density on passing to the amorphous phase in YIG. After the calculation of densities and packing fractions in Sec. II we pass to a point-charge calculation of the electric field gradient (EFG) at the iron sites in Sec. III. The larger value of d for FeF_3 leads to a better packing of anions around an average iron (though not to a larger number of actual contact anions) and results in a smaller EFG distribution width and hence a smaller quadrupole splitting than in amorphous YIG, in agreement with the observed Mössbauer measurements.

In Sec. IV we compute the correlation functions for iron-iron, iron-fluorine, and fluorine-fluorine pairs out to a range of 10 Å. Identifiable details of local structure are recognizable out to a larger range than was possible for the computer YIG model, indicating a higher degree of local order in FeF_3. This is partly due to the larger d value but also to the fact that the ratio of the F to Fe ionic radii (determined from the crystalline FeF_3 lattice) is almost perfect for the packing of six fluorines around one iron.

In Sec. V we examine the details of local structure, bond angles, and coordination, and relate

them where possible to magnetic properties. Although an almost perfect six-packing of fluorines around iron is found close to the seed cluster of the computer sample, this feature is somewhat less pronounced in the main body of the "sample." We compute, in particular, the angular distribution of nearest-neighbor iron–fluorine–iron bonds and infer the distribution of exchange energy which results from those cations which are essentially in contact with the same anion. Comparing these findings with magnetic measurements on the amorphous material, we find that significantly less than half the exchange energy in amorphous FeF_3 can be attributed to these nearest-neighbor (or "contact") pairs. By contrast, we find that most of the magnetic energy does arise from contact neighbors in amorphous YIG.

Both crystalline FeF_3 and crystalline YIG exhibit long-range magnetic ordering above room temperature while their amorphous equivalents undergo a "spin freezing" only at very low temperatures ($T \approx 30$ K). The amorphous ordered phase in both cases is probably speromagnetic, which involves an antiferromagnetic alignment on a local scale without the definition of sublattices. Our work suggests that the low ordering temperatures in amorphous FeF_3 and YIG may have somewhat different origins, being dominantly a frustration effect in the former but arising in YIG as a direct result of a low coordination number for strongly antiferromagnetic interactions.

II. THE COMPUTER MODEL

Details of the crystal structure of crystalline FeF_3 have been given by Hepworth *et al.*[7] Each ferric ion is equidistant some 1.92 Å from six fluorine anions which form an almost regular octahedron around it. Using the conventional ionic fluorine radius of $R(F) = 1.36$ Å establishes a ferric radius $R(Fe) = 0.56$ Å as appropriate for crystalline FeF_3. Our first assumption is that these radii remain appropriate for use in constructing a hard sphere model for amorphous FeF_3.

In constructing the model we follow closely the procedure set out in Ref. 5 for amorphous YIG but now, since we are concerned with a binary rather than a ternary system, we can dispense with the recipe for choosing between two types of cations in the sequential addition procedure. A seed cluster is formed from two fluorine spheres and one iron sphere all in contact in the xy plane, with one of the fluorine centers adopted as the origin [or more accurately as the point $(0, 0, 10^{-5}$ Å), a procedure which removes $(z, -z)$ symmetry around the seed and prevents the occurrence of pockets which are equidistant from the origin].

In adding spheres, our primary criterion is that no two cations shall touch or indeed come closer than an initially arbitrary center-to-center distance $d > 2R(Fe)$. Starting from the seed we compute the possible positions (pockets) of a new fluorine sphere in contact with the three spheres of the seed (the first pockets must be anion pockets since they involve contact with a cation). Thus the seed-pocket calculation results in a substrate of $N = 3$ ions and the positions of $M = 2$ new sites for an additional anion. Labeling all substrate ions and pockets by their formal valence charges ($F = -1$, $Fe = +3$), the following procedure is now general for general N and M.

We first choose the pocket nearest to the origin (the "global" pocket) and fill it as long as it does not result in a violation of the d criterion. If it does, we strike out this pocket and proceed to the next global pocket until one is found which does not violate this criterion. After filling this pocket we strike out all pockets which overlap the added $(N+1)$th sphere and compute the newly created pockets involving this sphere. If a newly created pocket involves contact with a cation, then it is designated a fluorine pocket; if not, the pocket type (F or Fe) is decided by summing the valence charge on the existing substrate and adding that pocket which tends toward establishing charge neutrality. After calculating all new pockets, we strike out those which overlap the existing substrate. We now redefine N and M to represent the new substrate and pocket sets and repeat the entire procedure.

If the distance d is too large, M goes to zero at some stage of the building process and the procedure terminates. The largest value of d for which the building program will propagate in some sense therefore minimizes the local Coulomb energy within the building algorithm. This value of d is found by trial and is $d = 2.7$ Å in FeF_3 compared with $d = 2.4$ Å in YIG.[5] With $d = 2.72$ Å, building ceases at $N = 6$ so that the exact value of d for FeF_3 is between 2.70 and 2.72 Å. We have used $d = 2.70$ Å to construct a cluster of 858 ions with cluster size limited only by computer-time restriction.

This approximately spherical "computer sample" of amorphous FeF_3 is 27.4 Å in diameter and contains $N(Fe) = 215$ cations and $N(F) = 643$ anions, giving a ratio $N(Fe)/[N(Fe)+N(F)] = 0.251$ to be compared with the ideal 0.250. However, since $R(Fe)$ is small compared to $R(F)$, occasional pockets for Fe are created and immediately filled as much as 1.8 Å inside the "surface" of the cluster, tending to make the surface region slightly iron deficient and the rest of the cluster very slightly iron rich. With $d = 2.7$ Å, the smallest

allowed Fe–F–Fe bond angle θ_{min} is very close to 90° (actually 89.4°) and is considerably larger than its equivalent (i.e., Fe–O–Fe) $\theta_{min} = 76°$ in computer model amorphous YIG.[5]

Plotting the surface radius of the cluster sample $r(N)$, defined by the radial coordinate of the fairly smoothly varying anions alone as a function of $1/N$, we can graphically extrapolate to $1/N \to 0$ to obtain the reciprocal atomic density

$$\rho^{-1} = \lim_{1/N \to 0} [4\pi r^3(N)/3N] = (12.80 \pm 0.15)\ \text{Å}^3 \quad (1)$$

(per atom) for amorphous FeF_3. This compares with the equivalent crystalline value[7] of 13.00 Å^3 and suggests a possible slight increase in density in going to the amorphous phase. This result is to be contrasted with the YIG situation[5] where a decrease of density of some 5% was suggested by the same model on passing to the amorphous phase. The difference is due both to a more efficient packing of FeF_3 in the glass and a less efficient packing in the crystal. Quantitatively the effect is expressed by packing-fraction calculations as shown in Table I where we also show other data comparing the FeF_3 and YIG systems.

III. EFG AT THE IRON SITES

A particularly useful probe of local structure in amorphous materials containing Mössbauer nuclei is the Mössbauer quadrupole spectrum. In FeF_3, above the spin-freezing temperature ~ 30 K, a simple two-line spectrum is expected and observed for the ^{57}Fe quadrupole resonance.[3] The splitting and line shape measure indirectly the distribution of electric-field gradients at the iron sites. The latter can be computed from the model of Sec. II in a point-charge approximation as described (for the analogous YIG model) in Ref. 5. Using formal valence charges $z(Fe) = +3$ and $z(F) = -1$, we compute directly the principal

TABLE I. Comparison of ionic radii R, minimum cation-cation distance d, minimum iron-anion-iron angle θ_{min}, packing fraction f, and reciprocal ionic density ρ^{-1} in FeF_3 and YIG.

	FeF_3	YIG
R(Fe) (Å)	0.56	0.54
R(anion) (Å)	1.36	1.40
R(Y) (Å)		1.00
d (Å)	2.7	2.4
θ_{min} (deg)	89	76
f(crystal)	0.622	0.649
f(amorphous)	0.632	0.618
ρ^{-1}(crystal) (Å^3 per ion)	13.00	11.85
ρ^{-1}(amorphous) (Å^3 per ion)	12.80	12.45

EGF modulus $|V_{11}|$ and asymmetry parameter η at all Fe sites more distant than 3 Å from the cluster surface. We obtain the distributions shown in Figs. 1 and 2 in histogram form. From the innermost Fe sites in the cluster, the accuracy of truncating the EFG radial summation can be estimated. We find that an rms error of ~± 0.13 e/Å^3 is incurred (where e is electronic charge) for a 3 Å truncation and ~± 0.06 e/Å^3 for a 4 Å cutoff.

From the Fig. 1 histogram we see that the $|V_{11}|$ distribution $p(|V_{11}|)$ is essentially zero at $V_{11} = 0$, peaks at or a little above 0.3 e/Å^3, and falls back to very small values above 0.7 e/Å^3. The peak value V_M and distribution width are both smaller than their equivalents [Fig. 2(c) of Ref. 5] in YIG. Experimentally, the peak-to-peak quadrupole splitting (QS) for amorphous FeF_3 is found[3] to be ~ 0.54 mm/sec compared with 1.05 mm/sec for YIG. From Fig. 1 we expect that a reasonable analytic representation for the EFG distribution might be a (possibly asymmetric) Gaussian.[8] We therefore write this distribution as

$$p(|V_{11}|) = \begin{cases} A_1 \exp\{-[(|V_{11}| - V_M)/aV_M]^2\}, & |V_{11}| < V_M \\ A_1 \exp\{-[(|V_{11}| - V_M)/bV_M]^2\}, & |V_{11}| > V_M \end{cases} \quad (2)$$

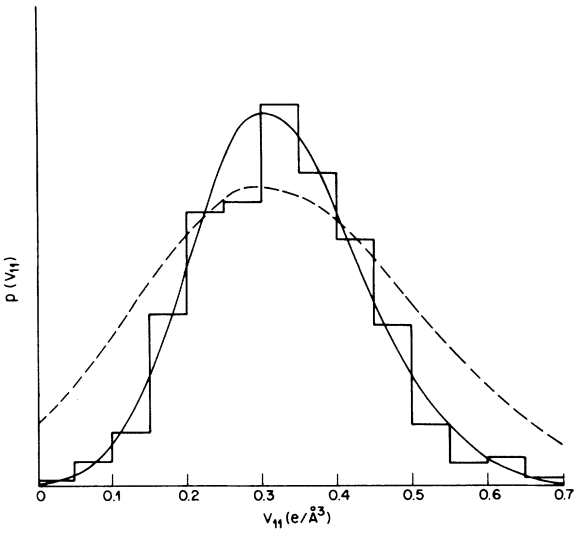

FIG. 1. Histogram for the probability distribution $p(|V_{11}|)$ of iron site principal EFG matrix elements $|V_{11}|$ calculated from the computer model in a point-charge approximation. Also shown for comparison are the asymmetric Gaussian distributions which result from fitting the QS line shape via Eq. (3). The dashed curve arises from the use of a natural Lorentzian line width $w = 0.20$ mm/sec in (3), and the solid curve from putting $w = 0.38$ mm/sec (see text).

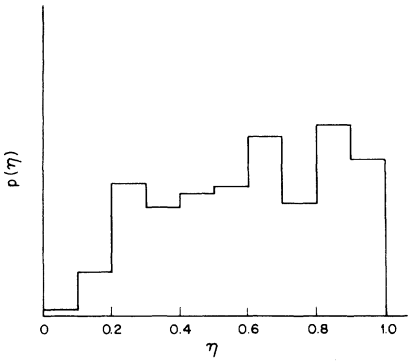

FIG. 2. Histogram of the probability distribution $p(\eta)$ of the EFG asymmetry parameter η from the computer model point-charge EFG calculation.

in which a and b are dimensionless parameters measuring distribution width. In terms of this distribution we calculate a Lorentz-broadened symmetric doublet line shape in the form

$$f(y) = A_2 \int_{-\infty}^{\infty} \frac{(w/2)^2 \exp\{-[(|V_{11}| - V_M)/xV_M]^2\} dV_{11}}{(w/2)^2 + (y - V_{11})^2}, \tag{3}$$

where A_2 is an amplitude factor, y runs between $-\infty$ and ∞, w is the full Lorentz width at half maximum, and x takes the value $a(b)$ when $|V_{11}|$ is smaller (greater) than V_M, the latter parameter being defined as positive.

The correct value to be used for w is uncertain,[9] although it must be greater than $w = 0.20$ mm/sec, corresponding to a natural linewidth, and less than $w = 0.38$ mm/sec, the width observed[3] for the (possibly split but unresolved) closely Lorentzian single-line quadrupole spectrum of paramagnetic crystalline FeF_3. Using Eq. (3) we show in Fig. 3

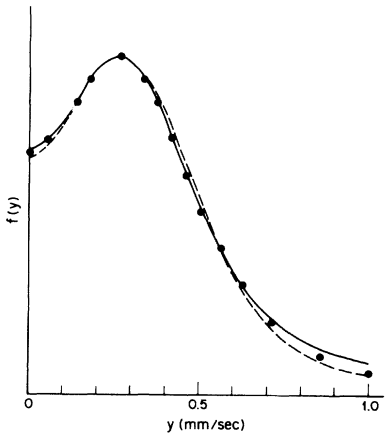

FIG. 3. Best theoretical fits [using Eq. (3)] to the experimental Mössbauer line shape (filled circles; data taken from Ref. 3). The solid and dashed curves correspond to their counterparts in Fig. 1.

the separate best fits to the amorphous QS data[3] obtainable with these two extreme values for w. The parameter values defining these fits are, respectively,

$$\begin{aligned} &\text{(A)} \quad w = 0.20 \text{ mm/sec}, \quad a = 0.80, \\ &\qquad b = 0.95, \quad V_M = 0.27 \text{ mm/sec}, \\ &\text{(B)} \quad w = 0.38 \text{ mm/sec}, \quad a = 0.45, \\ &\qquad b = 0.60, \quad V_M = 0.27 \text{ mm/sec}. \end{aligned} \tag{4}$$

The uncertainty involving w is of much greater significance for FeF_3 than it was for YIG because of the much narrower QS in the former case. In Ref. 5 the QS-fit for YIG was performed with the natural linewidth $w = 0.20$ mm/sec, although later more detailed study[8] suggested that a somewhat larger value optimized the fit.

In Fig. 1 we show the distributions $p(|V_{11}|)$ $a = 0.80$, $b = 0.95$ (dashed curve) and $a = 0.45$, $b = 0.60$ (full curve), compared with the computer histogram. Both the QS-fits of Fig. 3 and the histogram comparison of Fig. 1 suggest that the appropriate value for w in the experimental context of Ref. 3 should be closer to 0.38 than 0.20 mm/sec. The former value provides an excellent fit to the computer EFG histogram if $V_M = 0.30$ $e/\text{Å}^3$. The relationship between the QS units (mm/sec) and the EFG units ($e/\text{Å}^3$), using the most accurately available values for nuclear quadrupole moment and Sternheimer antishielding factor,[10,11] is (see Ref. 5)

$$1(e/\text{Å}^3) \approx 1.35 \text{ mm/sec}, \tag{5}$$

so that the computer EFG leads to a value $V_M = 0.30 \times 1.35 = 0.40$ mm/sec, to be compared with the observed $V_M = 0.27$ mm/sec of Eq. (4). Since the EFG calculation was performed with valence point charges, this formally would imply that effective point charges be reduced to some 70% of their valence values. Although this seems physically quite reasonable, the errors incurred in the hard-sphere aspects of the model and the point-charge aspects of the EFG calculation itself suggest that no quantitative significance yet be attached to such effects. For example, no reduction was found necessary for the equivalent YIG calculation,[5] although for a ternary system such as YIG, a single reduction parameter would not be appropriate in any case.

IV. THE PAIR-CORRELATION FUNCTIONS

In this section, again following the procedures set out in Ref. 5, we have computed the various pair-correlation functions for amorphous FeF_3 directly from the computer model cluster. For FeF_3 there are only three such independent func-

tions $g_{\alpha\beta}(r)$, which measure the average density of ions of type β at a distance r from ions of type α, since $g_{\alpha\beta}(r)$ and $g_{\beta\alpha}(r)$ are trivially related.[5] In Figs. 4, 5, and 6, we display, respectively, $g_{FeF}(r)$, $g_{FeFe}(r)$, and $g_{FF}(r)$, each out to a radius of ten angstroms.

As for YIG, certain obvious features of these correlations for comparatively short range r can be correlated with planar geometrical configurations of the hard-sphere components (see the figures). However, with the larger d value, the FeF_3 amorphous structure is "less randomly structured" on the local scale than YIG and details in the iron-fluorine and fluorine-fluorine functions are recognizable out to the third-neighbor "shell" with $r \sim 7$ Å. Statistics for the iron-iron function are less impressive than the others by virtue of the relatively small number of Fe-Fe pairs in the sample compared to Fe-F or F-F pairs. One significant feature in the $g_{FeF}(r)$ histogram at $r = 3.4$ Å is not a planar feature but is readily identified as a simple three-dimensional configuration obtained by adding a fluorine-contact sphere to the planar configuration indicated in Fig. 5 for the Fe-Fe function at $r = 2.7$ Å.

We note from the amplitude (0.832) of the 0.1-Å wide "contact spike" at 2.9–3.0 Å in Fig. 4 that approximately 3.9 fluorine ions "contact" an average ferric ion. This is almost exactly the same figure (3.8) calculated from the iron-oxygen contact spike in YIG (Fig. 8 of Ref. 5) for the number of oxygen ions in contact with an average ferric ion in amorphous YIG. In spite of this similarity there are, in fact, some interesting differences

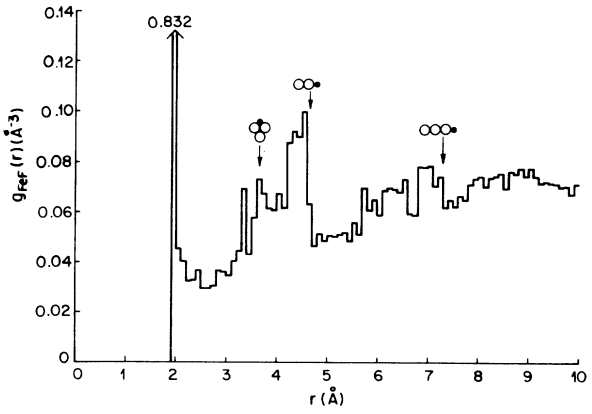

FIG. 4. The pair correlation function $g_{FeF}(r)$ which measures the density of fluorine ions at a distance r from an iron ion, as determined directly from the computer sample. Shown in this and the other pair correlation figures are r values corresponding to simple planar geometric configurations of the constituent hard spheres as illustrated, where open circles represent F ions and closed circles represent Fe ions.

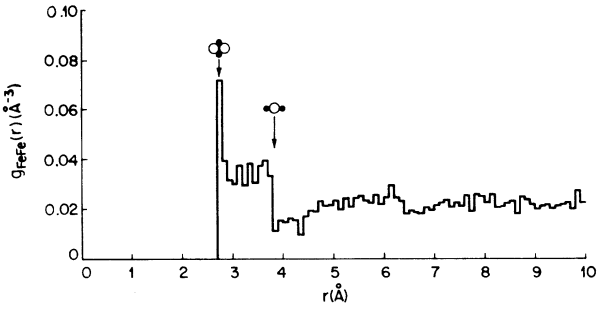

FIG. 5. As Fig. 4 but for correlations $g_{FeFe}(r)$ of iron-iron density.

in local iron-anion-iron coordination between the two amorphous models, and these will be set out in the following section.

V. LOCAL COORDINATION AND MAGNETIC PROPERTIES

Crystalline FeF_3 is a weak ferromagnet[12] with dominant exchange forces which are strongly antiferromagnetic[13] arising from kinetic superexchange via Fe–F–Fe single-bridge anion ligands with a bond angle (at the anion site) of $\theta_{cryst} = 153°$.[7] Each ferric ion in the crystal couples equally to six iron nearest neighbors and produces, below the Néel temperature, a simple two sublattice antiferromagnetic structure (neglecting the small canting) with coordination number $z = 6$, i.e., essentially a simple cubic antiferromagnet.

The crystalline Néel temperature is $T_N = 363$ K and the reported Curie-Weiss constant is $\Theta_C = -610$ K.[14] Since the crystal structure seems to preclude the possibility of significant exchange from other than nearest neighbors, we can use the series expansion formula for a six-coordinated two-sublattice antiferromagnet,[15] viz.,

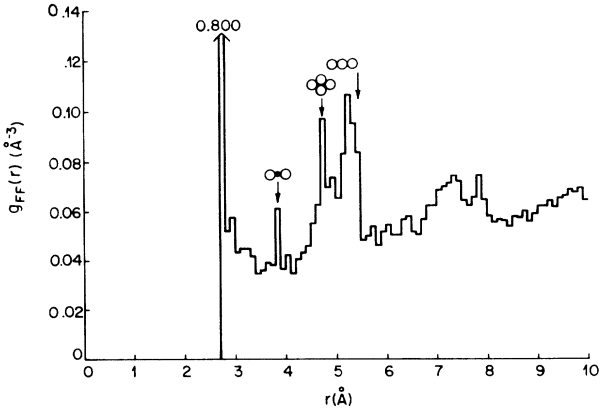

FIG. 6. As Fig. 4 but for correlations $g_{FF}(r)$ of fluorine-fluorine density.

$$-kT_N = (50J/192)[11S(S+1) - 1] \times \{1 + [0.10/S(S+1)]\}, \quad (6)$$

to extract the exchange constant J (defining J by a pair exchange $-2J\vec{S}_i \cdot \vec{S}_j$) for the crystal. Putting $S = \frac{5}{2}$ in Eq. (6) leads to $J = -14.5$ K. Using the Curie-Weiss relationship $12JS(S+1)/3 = -610$ K, on the other hand, gives an estimate $J = -17.4$ K. For high-temperature antiferromagnets of this type, such a discrepancy is common and usually results when the experimental Θ_C is extracted from data for which T/T_N is not sufficiently large for the simple Curie-Weiss relationship to be rigorously valid. For our purposes, however, $J(\text{crystal}) \approx -16$ K will be quite sufficient.

Amorphous FeF_3 is magnetically very different[3] from its crystalline counterpart. Although it has a high value of Curie-Weiss constant $\Theta_g = -486$ K, suggesting a dominance of antiferromagnetic forces, it does not exhibit a sharp magnetic transition at any temperature although a gradual spin freezing to an amorphous antiferromagnetic (termed speromagnetic[16]) phase takes place at $T_N \approx 28$ K.

In the computer model for amorphous FeF_3 there exists a complete spectrum of iron-fluorine-iron bond angles θ between about 90° and 180°. To examine this bond-angle distribution $p(\theta)$, we have sampled all pairs of iron spheres which touch a common fluorine sphere and for which at least one iron is less than 9 Å from the sample origin (to avoid surface effects). The result, in histogram form, is shown in Fig. 7. Two differences from the equivalent distribution in YIG (Fig. 12 of Ref. 5) are noted. First, since the minimum value of θ in amorphous FeF_3 is only a fraction of a degree less than 90° (89.4° to be precise), and double-bridging requires $\theta < 89.8°$, extremely few of the iron ions are double-bridged in FeF_3, whereas a significant fraction were[5] in YIG. Second, we note in the FeF_3 model (but not to anything like the same extent in YIG) that the iron ions close to the origin (i.e., close to the seed cluster) of the sample are atypical, with a much higher local degree of close-packing than the rest. They have, for example, in addition to four contact fluorines, two other fluorines (which I term neocontact) for which the Fe-F distance is ≤ 2.0 Å (contact distance being 1.92 Å). Thus, they are all approximately six-coordinated whereas, farther out in the cluster, the iron coordination (including neocontact out to 2 Å) is dominantly four (59%) and three (39%) with very few examples of five and six coordination. The effect is probably the result of having a high-symmetry seed together with a sphere-radius ratio $R(\text{Fe})/R(\text{F}) = 0.412$ which is extremely close to the packing ratio

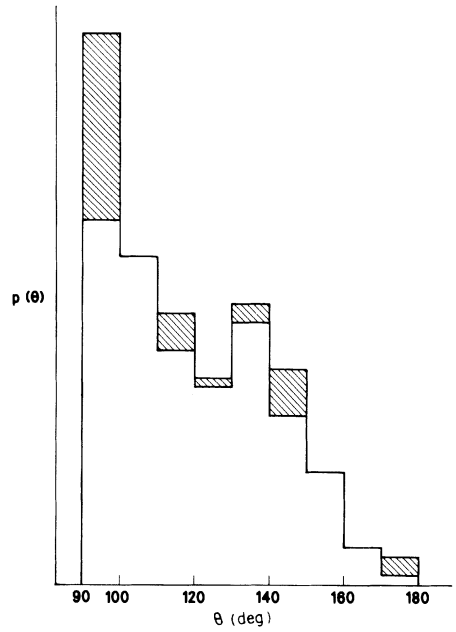

FIG. 7. Histogram of the probability distribution $p(\theta)$ of Fe–F–Fe bond angles θ within the computer "sample." We have shaded contributions (see text) which arise from an atypical core section defined here as involving at least one iron closer than 4 Å to the origin of the sample.

$(\sqrt{2} - 1)/1 = 0.414$, which would enable six F to perfectly pack one Fe. Because of this situation, we have marked separately (shaded) in Fig. 7 (and in Fig. 8 to follow) those contributions which come from irons closer than 4 Å to the origin.

In Fig. 8 we examine the distribution of nearest-neighbor magnetic ions defined as cations in actual contact or neocontact (separation < 2 Å) with a common anion. We compute, in particular, the probability $p(n)$ that a ferric ion has n magnetic nearest neighbors and the results for actual contact pairs (labeled contact) and for contact *plus* neocontact pairs (labeled neocontact) are separately displayed. Also in Fig. 8 we show the equivalent distribution $p'(n)$ of all iron nearest-neighbor pairs with a bond angle $\theta > 115°$. These, as discussed in Ref. 5, are the pairs which are likely to be strongly coupled antiferromagnetically. Thus, the most probable number of iron-pair nearest-neighbors (including neocontact) of a particular cation is four, with two or three of them strongly coupled antiferromagnetically. This leads to a certain amount of "frustration" (iron triads interacting antiferromagnetically). Some of the more significant of these results, compared with their equivalents for YIG, are given in Tables II and III. In particular, from Table III, which tabulates data relevant for a discussion of frustration, we see that the density of frustrated triads in both

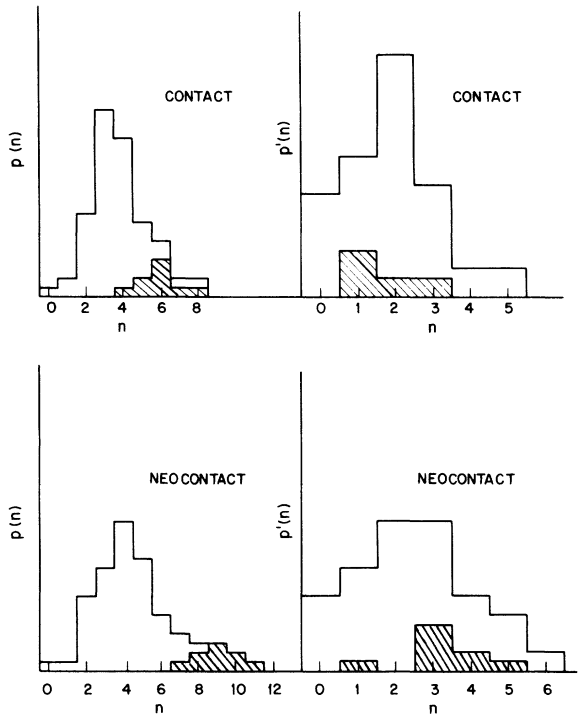

FIG. 8. The probabilities $p(n)$ and $p'(n)$ that a magnetic ion in the amorphous FeF_3 computer sample has, respectively, n single-anion-bonded magnetic nearest neighbors and n such neighbors with a bond angle θ greater than 115°. The latter are those which are strongly magnetically interacting. The pair of histograms labeled "contact" include only those cation spheres which literally touch a common anion sphere (contact radius 1.92 Å). The histograms labeled "neocontact" include also those noncontact pairs for which the cation-anion center-to-center distance is less than 2 Å. We have again shaded, as in Fig. 7, contributions arising from the atypical core section of the sample.

FeF_3 and YIG is quite small if iron-anion distances <2 Å are deemed essential for strong exchange. If this restriction is relaxed, however (and this point will be discussed further below), Table III shows that frustration in amorphous FeF_3 increases rapidly as a function of iron-anion distance whereas that in amorphous YIG does not.

Comparisons with YIG are now instructive. Crystalline YIG has a Curie temperature of 559 K and an iron–oxygen–iron bond angle $\theta_{cryst} = 127°$. The dominant exchange has been calculated by Wojtowicz[17] and found to be J (crystal) ≈ -33 K. If we assume that the contact bonding in the glass and in the crystal is similar, then we would anticipate that J (glass) at $\theta = \theta_{cryst}$ would be of the order J(crystal), both in FeF_3 and YIG. Since the angular dependence of ferric exchange is known[18] for larger values of θ, viz., $J(\theta) \propto \cos\theta$, this suggests maximum values of J (i.e., for $\theta = 180°$)

TABLE II. Comparison of magnetic and crystalline data for FeF_3 and YIG. The last three entries are calculations from the computer model in regions well removed from the "seed cluster."

	FeF_3	YIG
Fe–anion–Fe bond angle θ (crystal)	153°	127°
T_N (crystal)	363 K	559 K
T_N (glass)	~30 K	~30 K
Curie-Weiss constant (glass)	−486 K	−500 K
Magnetic coordination number (crystal)	6	5 (average)
Nearest-neighbor exchange J (crystal)	−16 K	−33 K
180° nearest-neighbor exchange J_{max}(glass)	~−18 K	~−55 K
Fe–anion contact distance (glass)	1.92 Å	1.94 Å
% iron with contact anion coordination number n	$n=3$ (48%) $n=4$ (52%)	$n=3$ (28%) $n=4$ (72%)
% iron with n anions closer than 2 Å (neocontact)	$n=3$ (39%) $n=4$ (59%) $n=5$ (2%)	$n=3$ (26%) $n=4$ (74%) $n=5$ (0%)
% iron with n anions closer than 2.4 Å	$n=3$ (0%) $n=4$ (45%) $n=5$ (45%) $n=6$ (10%)	$n=3$ (10%) $n=4$ (50%) $n=5$ (38%) $n=6$ (2%)

in the amorphous materials of order $J_{max} = -18$ K (FeF_3) and $J_{max} = -55$ K (YIG). Now the reported values of the Curie-Weiss constant Θ_g are essentially the same (≈ -500 K) for each. This enables us to extract an average exchange energy (where z is the number of magnetic neighbors),

TABLE III. A comparison of "frustration" in the computer models for FeF_3 and YIG. Defining as frustrated all iron atoms involved in magnetic triads for which all three exchange pairs are strongly antiferromagnetically coupled ($\theta > 115°$), we have computed the number N_R of frustrated triads involving at least one of the innermost 100 iron atoms and also the number N_F of frustrated atoms in this 100 iron atom core. Results are given for several different values of iron-anion "bond length" D, assuming in each case that strong magnetic superexchange can result only if the cation-anion distance is less than or equal to D.

	FeF_3			YIG	
D (Å)	N_R	N_F	D (Å)	N_R	N_F
contact (1.92)	5	12	contact (1.94)	5	8
2.0	11	19	2.0	5	8
2.2	15	26	2.2	6	9
2.4	18	29	2.4	7	9

$$\overline{zJ} = 3\Theta_g/[2S(S+1)] \approx -85 \text{ K}, \quad (7)$$

leading to

$$\overline{zJ}/J_{max} \approx 4.7 \ (FeF_3), \quad \overline{zJ}/J_{max} \approx 1.5 \ (YIG). \quad (8)$$

For contact iron pairs we can determine from the computer model the bond angle θ distribution of neighbors at each iron site. Since the qualitative form for exchange distribution $J(\theta)$ as a function of θ is known for ferric ions[5] [see Fig. 9(a)], we can therefore compute $\sum J(\theta)/J_{max}$ for each iron site. The resulting distribution, which we term $p(zJ_{eff})$, as a function of zJ_{eff}/J_{max} is shown in Fig. 9(b). The calculation is actually performed for contact *plus neocontact* pairs, which we term nearest-neighbor (NN) pairs. The mean value of this distribution along the abscissa defines an average exchange energy per site, which we designate $\overline{zJ}$, in units of J_{max}. We find, where we include also the result of an analogous calculation for YIG,[19]

$$(\overline{zJ}/J_{max})_{NN} \approx 1.6 \ (FeF_3), \quad (\overline{zJ}/J_{max})_{NN} \approx 1.2 \ (YIG), \quad (9)$$

where the subscript NN reminds us that Eqs. (9) are relevant only for nearest neighbors as defined above. The smaller YIG value results primarily from the larger concentration of ferromagnetic pairs ($74° \lesssim \theta \lesssim 100°$) in YIG. Comparing Eqs. (8) and (9), a striking difference between amorphous YIG and amorphous FeF_3 emerges, whereas ~80% of the magnetic energy in amorphous YIG arises from nearest neighbors, only ~35% of that in amorphous FeF_3 does.

This implies that whereas a contact model (including exchange only between iron pairs actually in contact, or neocontact, with a common anion) is likely a fairly valid model for amorphous YIG, it almost certainly is not adequate for amorphous FeF_3. We can, in fact, within the computer models, see the origin of this difference. In YIG, with a contact distance for Fe–O of 1.94 Å, only 2% of the iron cations possess additional noncontact anions closer than 2 Å (i.e., neocontact anions) and only 20% possess noncontact anions closer than 2.2 Å. The equivalent figures for FeF_3 are 13% and 53%, respectively (excluding the atypical "seed" region for which these values are even larger). Thus, if significant exchange interactions can occur between iron pairs with Fe-anion separations up to, say, 10–15% larger than contact (which from the above calculation now seems likely), then the fraction of exchange energy coming from "noncontact" pairs will be very significantly greater for FeF_3 than for YIG.

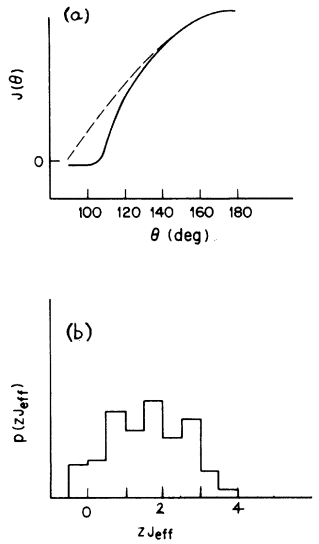

FIG. 9. (a) The qualitative form expected for Fe–F–Fe superexchange $J(\theta)$ as a function of bond angle θ. The dashed curve is proportional to $\cos\theta$ and is the form expected to be valid (Ref. 18) for the larger bond angle values. (b) The distribution $p(zJ_{eff})$ of the sum of exchange $\Sigma J(\theta) \equiv zJ_{eff}$ over all contact and neocontact bonds at each iron site. The abscissa units are $J_{max} = J(\theta = 180)$.

We conclude, finally, that the low-ordering temperatures $T_N \sim 30$ K reported for both amorphous FeF_3 and YIG may have somewhat different origins. Since the contact model seems fairly adequate for YIG the discussion given in Ref. 5 remains valid for this material, with the low T_N resulting from a low coordination number for strongly antiferromagnetic interactions [Eq. (8)]. In this picture a resemblance to dilute antiferromagnetism is suggested[5] and frustration (Table III) plays a minor role at best. In FeF_3, by reason of the large number of strongly magnetic noncontact neighbors, the effective coordination number for strongly antiferromagnetic neighbors is much higher [Eq. (8)]. From Table III we see that this situation leads to a much larger potential for frustration. If, for example, iron-anion bond lengths up to 2.4 Å can be included in the exchange network then (Table III) close to 30% of the spins may be frustrated in FeF_3. This number increases to 40% if we include bond angles to $\theta \approx 110°$. Since the truly relevant quantity is the percentage of frustrated spins in the "infinite cluster" and not in the total assembly, these numbers should perhaps be even higher, suggesting that frustration may well be the primary mechanism responsible for the low magnetic ordering temperature in amorphous FeF_3.

[1]F. J. Litterst, J. Phys. (Paris) 36, L197 (1975); F. J. Litterst, G. M. Kalvius and A. J. F. Boyle, in *Magnetism and Magnetic Materials—1973 (Boston)*, Proceedings of the 19th Annual Conference on Magnetism and Magnetic Materials, edited by C. D. Graham and J. J. Rhyne (AIP, New York, 1974), p. 616; J. Phys. (Paris) 35, C6-403 (1974).

[2]E. M. Gyorgy, K. Nassau, M. Eibschutz, J. V. Waszczak, C. A. Wang, and J. C. Shelton, J. Appl. Phys. 50, 2883 (1979).

[3]G. Ferey, A. M. Leclerc, R. de Pape, J. P. Manot, and F. Varret, Solid State Commun. 29, 477 (1979).

[4]G. Ferey, F. Varret, and J. M. D. Coey, J. Phys. C 12, L531 (1979).

[5]M. E. Lines, Phys. Rev. B 20, 3729 (1979).

[6]C. H. Bennett, J. Appl. Phys. 43, 2727 (1972).

[7]M. A. Hepworth, K. H. Jack, R. D. Peacock, and G. J. Westland, Acta Crystallogr. 10, 63 (1957).

[8]Deviations from Gaussian form have recently been established by a nonlinear least-squares fit to amorphous YIG Mössbauer quadrupole data [M. Eibschutz, M. E. Lines, and K. Nassau, Phys. Rev. B 21, 3767 (1980)], but the quality of the QS data in Ref. 3 is not high enough to enable such a careful analysis to be carried out at this time for amorphous FeF_3.

[9]Line broadening ($w > 0.20$ mm/sec) can occur as the result of several physical processes including Doppler effects, saturation in thick samples, strain broadening, and instrumental problems (nonlinear drive).

[10]S. N. Ray and T. P. Das, Phys. Rev. B 16, 4794 (1977).

[11]S. N. Ray, T. Lee, T. P. Das, R. M. Sternheimer, R. P. Gupta, and S. K. Sen, Phys. Rev. A 11, 1804 (1975).

[12]L. M. Levinson, J. Phys. Chem. Solids 29, 1331 (1968).

[13]E. O. Wollan, H. R. Child, W. C. Koehler, and M. K. Wilkinson, Phys. Rev. 112, 1132 (1958).

[14]J. M. Dance, Thèse de 3ème Cycle (Bordeaux 1973) (unpublished).

[15]G. S. Rushbrooke and P. J. Wood, Mol. Phys. 6, 409 (1963).

[16]J. M. Coey, J. Appl. Phys. 49, 1646 (1978).

[17]P. J. Wojtowicz, Phys. Lett. 11, 18 (1964).

[18]D. Treves, M. Eibschutz, and P. Coppens, Phys. Lett. 18, 216 (1965).

[19]M. E. Lines (unpublished).